Journal Pre-proof

Multiscale spatiotemporal meteorological drought prediction: A deep learning approach

Jia-Li ZHANG, Xiao-Meng HUANG, Yu-Ze SUN

PII: S1674-9278(24)00053-4

DOI: https://doi.org/10.1016/j.accre.2024.04.003

Reference: ACCRE 520

To appear in: *Advances in Climate Change Research*

Received Date: 18 September 2023

Revised Date: 18 January 2024

Accepted Date: 2 April 2024

Please cite this article as: ZHANG, J.-L., HUANG, X.-M., SUN, Y.-Z., Multiscale spatiotemporal meteorological drought prediction: A deep learning approach, *Advances in Climate Change Research*, https://doi.org/10.1016/j.accre.2024.04.003.

Multiscale spatiotemporal meteorological drought prediction: A deep learning approach

Jia-Li ZHANG, Xiao-Meng HUANG *, Yu-Ze SUN

Department of Earth System Science, Ministry of Education Key Laboratory for Earth System Modelling, Institute for Global Change Studies, Tsinghua University, Beijing 100084, China

Corresponding author: hxm@tsinghua.edu.cn (HUANG X.-M.)

Multiscale spatiotemporal meteorological drought prediction: A deep learning approach

Jia-Li ZHANG, Xiao-Meng HUANG *, Yu-Ze SUN

Department of Earth System Science, Ministry of Education Key Laboratory for Earth System Modelling, Institute for Global Change Studies, Tsinghua University, Beijing 100084, China

Corresponding author: hxm@tsinghua.edu.cn (HUANG X.-M.)

Abstract

Reliable monitoring and thorough spatiotemporal prediction of meteorological drought are crucial for early warning and decision-making regarding drought-related disasters. The utilisation of multiscale methods is effective for a comprehensive evaluation of drought occurrence and progression, given the complex nature of meteorological drought. Nevertheless, the nonlinear spatiotemporal features of meteorological droughts, influenced by various climatological, physical and environmental factors, pose significant challenges to integrated prediction that considers multiple indicators and time scales. To address these constraints, we introduce an innovative deep learning framework based on the shifted window transformer, designed for executing spatiotemporal prediction of meteorological drought across multiple scales. We formulate four prediction indicators using the standardized precipitation index and the standard precipitation evaporation index as core methods for drought definition using the ERA5 reanalysis dataset. These indicators span time scales of approximately 30 d and one season. Short-term indicators capture more anomalous variations, whereas long-term indicators attain comparatively higher accuracy in predicting future trends. We focus on the East Asian region, notable for its diverse climate conditions and intricate terrains, to validate the model's efficacy in addressing the complexities of nonlinear spatiotemporal prediction. The model's performance is evaluated from diverse spatiotemporal viewpoints, and practical application values are analysed by representative drought events. Experimental results substantiate the effectiveness of our proposed model in providing accurate multiscale predictions and capturing the spatiotemporal evolution characteristics of drought. Each of the four drought indicators accurately delineates specific facets of the meteorological drought trend. Moreover, three representative drought events, namely flash drought, sustained drought and severe drought, underscore the significance of selecting appropriate prediction indicators to effectively denote different types of drought events. This study provides methodological and technological support for using a deep learning approach in meteorological drought prediction. Such findings also demonstrate prediction issues related to natural hazards in regions with scarce observational data, complex topography and diverse microclimate systems.

Keywords: Meteorological drought; Spatiotemporal prediction; Multiscale; Swim transformer; Deep learning

1. Introduction

Meteorological drought is a complex natural phenomenon increasingly influenced by climate change (Manzano et al., 2019; Zhang et al., 2022), posing severe challenges to global water resource management and disaster prevention. Various forms of meteorological droughts can result from hydrological imbalances, such as inadequate rainfall and elevated evapotranspiration (Acharki et al., 2023; Alsubih et al., 2021). Contrary to rapid-onset disasters, meteorological droughts evolve and spread slowly across extensive spatial and temporal scales, manifesting strongly nonlinear dynamics (Mishra and Singh, 2010; Wu et al., 2022). Influenced by fluctuations in precipitation, temperature and other meteorological variables, the occurrence and severity of droughts are affected by diverse geographical factors, such as terrain, land-use patterns and soil conditions. Consequently, accurately modelling and predicting the intricate spatiotemporal evolution of meteorological droughts is challenging, particularly in regions with complex climatic and environmental systems (Li et al., 2021).

Great research efforts have been directed towards meteorological drought forecasting utilising station-based observations and gridded reanalysis products (Dikshit et al., 2022; Shen et al., 2019; Zhang et al., 2022). Several data-driven, physical and hybrid modelling techniques have been extensively employed for drought forecasting, covering multiple global and regional areas (Jamei et al., 2023). However, some prevalent limitations persist. Station-based predictions have limited spatial applicability and coverage (Hao et al., 2018). Although techniques, such as artificial neural networks, have been integrated (Alsubih et al., 2021; Azimi et al., 2023; Danandeh Mehr et al., 2023), the predictions often pertain only to local areas surrounding observation stations. They fail to apprehend detailed drought distributions and propagation over large heterogeneous regions (Dikshit et al., 2022; Jamei et al., 2023). Conversely, gridded reanalysis and model products support comprehensive drought monitoring and improved characterisation of complex spatiotemporal interactions (Zhang et al., 2022). Nonetheless, most studies have centred on single timescales or indicators, lacking a multifaceted and comprehensive assessment.

A single indicator facilitates the realisation of predictions. However, the effective quantification and indication of meteorological droughts, a natural disaster with complex causes, is still an advancing research topic (Dikshit et al., 2022). Researchers are committed to maximising the integration of hydro-meteorological and climatic variables into the quantification of meteorological drought or finding the most concise descriptive approach. However, regardless of the form utilised, prediction models relying on a single indicator can only account for one aspect, resulting in inevitably biased predictions. In addition, due to impacts from sudden climate events or outliers in data products, prediction results from single-indicator models lack robustness and are difficult to validate or refine through other approaches, indicating remaining reliability shortcomings.

Similarly, a single time scale is consistent with the general rules of model prediction. However, it

is often insufficient for various practical applications because large and small timescales tend to imply different information about drought. While long-term climate analyses can outline general drought trends, short-term extreme events, such as flash droughts, may be overlooked. Existing techniques also struggle in skilfully extracting and representing the elaborate spatiotemporal signatures of droughts, especially in regions with highly diverse terrain and microclimates. For instance, mountainous and plateau topographies can impede or partition moisture-laden air transported by monsoonal circulations, engendering microclimatic regimes that affect precipitation distribution and yielding significant disparities in wet and dry conditions. Moreover, transpiration differs across plains, high mountains and plateaus, attributable to variances in elevation, vegetative cover and edaphic environments. This condition further convolutes the spatial and temporal attributes of drought. Consequently, a powerful and reliable spatiotemporal prediction model is urgently required for interpreting meteorological drought by multi-timescales and multi-indicators.

Recently, transformer architectures have shown promising capabilities for spatiotemporal sequence modelling and forecasting (Vaswani et al., 2017). This typical architecture is predicated upon a sequence-to-sequence approach capable of linking contextual factors from the past to a prospective aim in the future. Transformers leverage self-attention and cross-attention as underlying building components. The advantages of the attention mechanisms in transformers lie in the capability of each token to engage with others and leverage semantic information more productively, rendering transformers adaptable for undertaking distant interconnectedness. Furthermore, multihead attention mechanisms capture spatial and temporal relations, enabling spatiotemporal predictions through explicit or implicit means. Essentially, the transformer architecture aligns with the objective of effective global–local spatiotemporal aggregation and has achieved outstanding results in Earth system prediction applications (Huang et al., 2022), including drought forecasting using climate indices (Duan and Zhang, 2022; Minixhofer et al., 2021). However, its application, where gridded data are directly used in complex regions, remains limited.

Therefore, an advanced transformer model is developed; it is specifically designed to exploit gridded meteorological data for multiscale drought prediction across topographically and climatically diverse regions. The flexibility of transformer architectures combined with physically meaningful data is expected to effectively enhance spatiotemporal drought analysis. The innovation of this study aims to overcome the limitations of traditional forecasting approaches that are constrained by a single indicator and time scale. The proposed method endeavours to expand the research perspective, thereby improving the robustness and practical applicability of meteorological drought predictions. Furthermore, the exploration of optimal approaches in constructing indices and time scales that cater to diverse needs is actively promoted. The ultimate goal is to provide concrete and reliable data support for the prevention of meteorological drought-related disasters.

The East Asian region is selected as the modelling domain, given the advantageous potential for validating model performance under complex climatic conditions. Previous studies have emphasised that expansive mountain chains, such as the Tibetan Plateau, the Kunlun, Himalayan and Andes Mountains in East Asia, considerably impact the existing global climate system (Kitoh, 2004). The interactions at myriad scales, including those involving oceanic and atmospheric circulation, are modified by these mountains, intensifying the challenge of analysing and predicting the behaviour of these variables when they intersect with mountainous terrains (Martens et al., 2020). Further complicating matters, the scarcity of observational data hinders pertinent research and forecasting applications. These issues underline the urgent necessity for precise and extensive drought forecasts derived from gridded meteorological data specific to this region.

2. Data and methods

2.1 Study region and dataset

The current research is centred on East Asia (3°–66°N and 75°–140°E). ERA5 products, developed by the European Centre for Medium-range Weather Forecasts, exemplify the latest progress in reanalysis technology. Prior research has confirmed that ERA5 precipitation data surpass several other products in accurately reflecting precipitation levels (Martens et al., 2020; Zhang et al., 2022; Torres-Vázquez et al., 2023). The two key variables utilised are hourly precipitation and 2-m temperature. We use half a century's worth of data, ranging from 1970 to 2020, at a horizontal resolution of 0.25° × 0.25°. The data gathered in 2020 form the basis for model testing and subsequent performance evaluations.

2.2 Drought indicators

The standardized precipitation index (SPI) is a globally approved drought index, which quantifies the probability of observed precipitation in comparison with long-term climatic conditions by fitting the precipitation data to a suitable probability distribution (McKee et al., 1995). The SPI offers flexibility because it can be used on any selected timescale, from daily measurements upwards. Thus, it has been extensively employed in meteorological drought studies.

The standard precipitation evaporation index (SPEI) (Vicente-Serrano et al., 2010) calculates the 'climatic water balance' using evapotranspiration and precipitation inputs. SPEI can be computed across various monthly timescales, ranging from 1 to 24 mon, thereby representing different types of droughts. Although the definitions of drought provided by SPI and SPEI coincide, their values may vary slightly due to differing underlying principles. Therefore, the combination of two indices to define drought is considered an objective and practical approach. Table 1 delineates the definition of drought

138 according to aridity indices, with positive (negative) values implying wet (dry) conditions.

139 Table 1 Classification of drought conditions according to SPI and SPEI indices (Rhee and Im, 2017).

Classification	Index value
Extremely wet	≥2.00
Very wet	1.50 to 1.99
Moderately wet	1.00 to 1.49
Near normal	0.99 to −0.99
Moderately drought	−1.00 to −1.49
Severe drought	−1.50 to −1.99
Extremely drought	≤−2.00

140 Drought is frequently assessed on a seasonal timescale to quantify precipitation trends over a
141 season (Hao et al., 2018). This scale carries physical and practical importance. Nevertheless, a one-
142 month accumulation window is applied, owing to the potential inadequacy of the seasonal scale in
143 indicating the rapid onset of meteorological drought. Ultimately, acknowledging the benefits of diverse
144 drought indices and timescales, SPI30 and SPI90 are selected to represent the single-month and
145 seasonal time scales, *i.e.* 30-d and 90-d accumulations. Meanwhile, SPEI-1 and SPEI-3 are designated
146 as the single-month and seasonal scales (3-mon), respectively.

147 **2.3 Drought prediction model**

148 This study aims to formulate a model equipped to amalgamate multiple indices to achieve
149 multiscale meteorological drought prediction. The widely utilised shifted window transformer (Swin
150 transformer) (Liu et al., 2021) serves as the foundational building block to enhance the model's
151 capability of spatiotemporal feature extraction. The Swin transformer uses hierarchical feature
152 representation and multiscale fusion, enabling the extraction of complex, interconnected features while
153 allowing the model to tackle dense prediction tasks.

154 Spatiotemporal variations within localised areas exhibit enhanced relevance because
155 meteorological droughts are impacted by regional geography and microclimatic systems. Consequently,
156 Swin transformers featuring localised attention and shift windowing are better positioned to accurately
157 and efficiently capture intrinsic spatiotemporal structural attributes. On the contrary, standard
158 transformers, which solely model global spatial relationships, tend to neglect such critical factors (Liu
159 et al., 2022). In addition to its applicability, Swin transformer has demonstrated its superior
160 performance and low computational complexity in the computer vision field, providing vital motivation
161 for adopting this backbone architecture in the current study.

162 Fig. 1 exhibits the structure of this multiscale meteorological drought prediction model, in which
163 the conventional U-net architecture with skip-connection is employed to fulfil the prediction task of the
164 model. Concurrently, the modules are designed in a 3D manner, ensuring that the data formatting
165 arrangement maintained within the model is spatiotemporal.

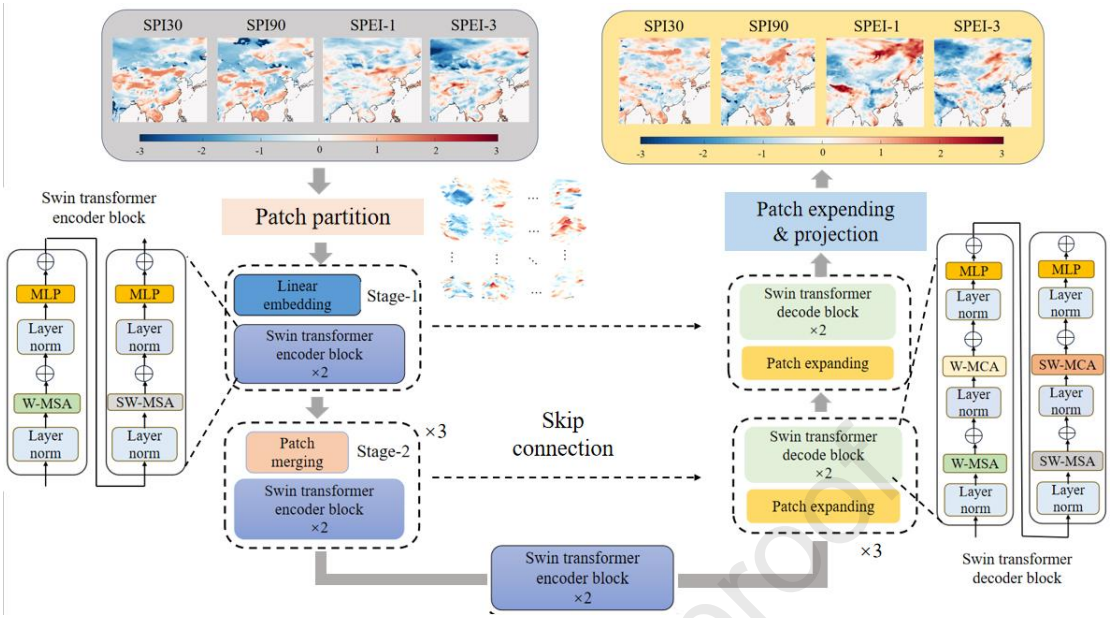

Fig. 1 Structure of the multiscale meteorological drought prediction model.

As depicted in Fig. 1, the gradual down-sampling in the encoder process undergoes multiple stages to capture salient local and global representations. Initially, the incoming data combination is segmented into small patches via a 3D patch partition layer. Subsequently, a linear embedding layer changes these patches to form the token for the subsequent Swin transformer block. Each Swin transformer encoder block uses two basic Swin transformer layers with differing interchange sliding windows: windowed multihead self-attention (W-MSA) and shifted window multihead self-attention (SW-MSA). The feed-forward network (MLP) and layer normalization are also incorporated as transformer layers, whereas the patch merging layer serves as a down-sampling operator to perform on incoming data. A neck block is established comprising two Swin transformer blocks to facilitate the connection between the encoder and decoder.

In the decoding process, multihead cross attention (MCA) is incorporated in addition to MSA. This approach aims to formulate the Swin transformer decoder block, thereby enabling an interaction between the encoded tokens and those being decoded. The patch expanding layer is employed as an up-sampling operation, corresponding to the patch merging layer applied to the decoder block. Contrary to the encoder blocks, the Swin transformers in decoder blocks, as shown in Fig. 1, leverage self and cross attention interchangeably, then shifted window self and cross attention. Through a series of Swin transformer decoder blocks, a patch expanding layer is employed for potential recovery of the spatial dimension that has been modified by the multistage encoder–decoder blocks. Lastly, the output of the final decoder block is processed by a fully connected layer. This layer allows the final results to be mapped to the target dimensionality and structure.

For any two attention layers in the Swin transformer block, the calculation process can be

expressed in Eq. 1 as follows:

$$\begin{cases} \hat{z}^{l} = W(L(z^{l-1})) + z^{l-1} \\ z^{l} = M(L(\hat{z}^{l})) + \hat{z}^{l} \\ \hat{z}^{l+1} = S(L(z^{l})) + z^{l} \\ z^{l+1} = M(L(\hat{z}^{l})) + \hat{z}^{l+1} \end{cases} \tag{1}$$

where W and S represent W-MSA and SW-MSA operator, respectively, M is the MLP module, $\hat{z}^{l}$ and z^{l} represent the output features of W-MSA and MLP module, respectively, and superscript l is the block number. As shown in Fig. 1, the W-MCA and SW-MCA modules are only added during decoding.

Fig. 2 presents the workflow of our proposed model for multiscale meteorological drought prediction, segmented into three phases: data processing, model training and model testing.

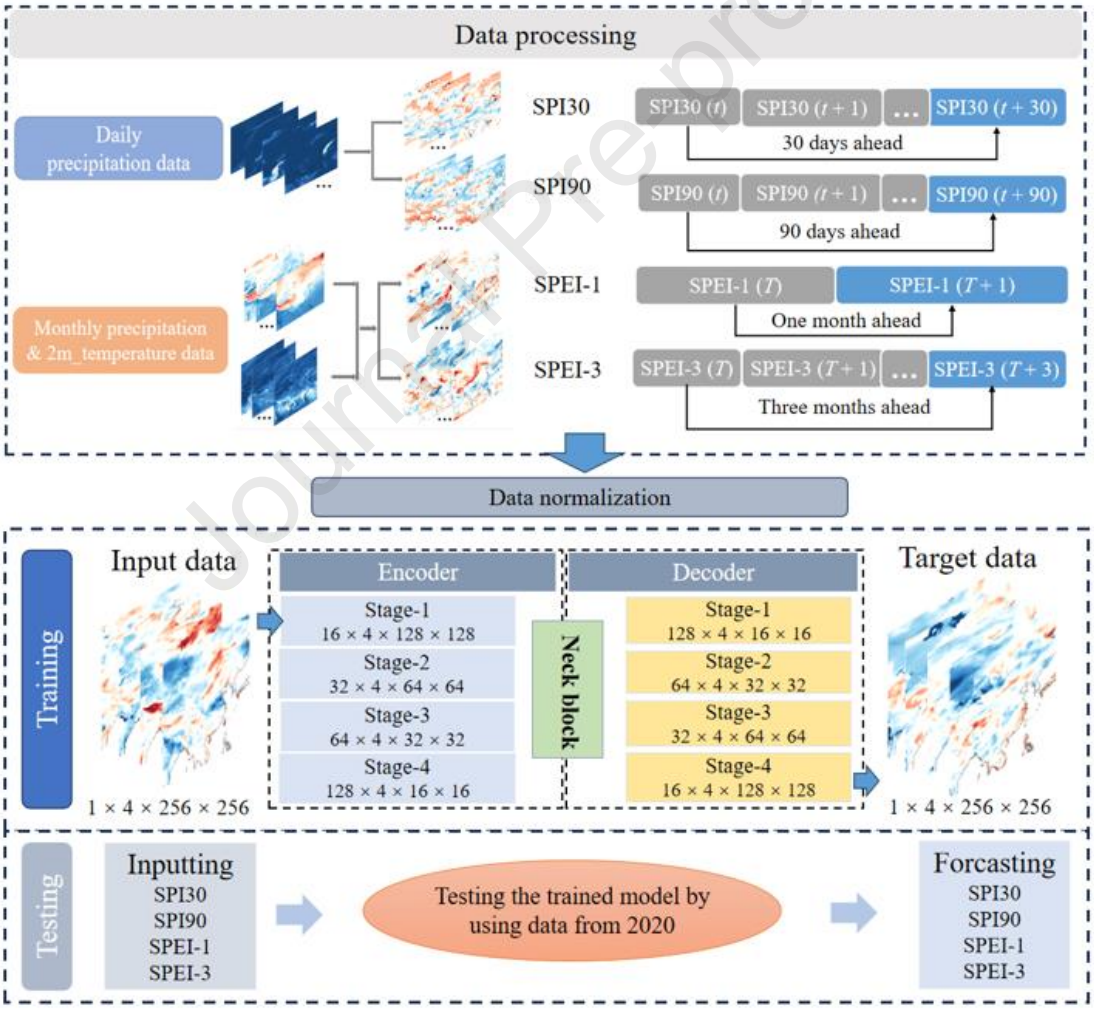

Fig. 2 Workflow for multiscale meteorological drought prediction.

The initial gridded precipitation and 2-m temperature data from ERA5 are provided on an hourly basis, necessitating their preprocessing. Precipitation data are processed into daily total precipitation and monthly aggregate precipitation, while the 2-m temperature information is transformed into

monthly averages. These modified data serve as the foundation for the computation of the multiscale drought indices. The data processing segment in Fig. 2 evidently shows that the daily precipitation frequency is utilised to derive SPI30 and SPI90, whereas the monthly aggregate precipitation and average temperature are employed to generate SPEI-1 and SPEI-3. The input data comprise a single set of four concurrent exponential values due to the differing temporal scales applied by SPI and SPEI. On the contrary, the target data correspond to the next temporal scale value of the four input indicators, implying that they do not occur simultaneously. The dataset necessary for model training and testing is constructed following these guidelines. Subsequent to the completion of the dataset construction, we also undertake normalisation processing on the data to facilitate efficient model training.

In the training phase, the input and output of the entire network are in a 3D tensor format, represented as [time_step, indicators_num, longitude, latitude]. The 'time_step' is set to 1, denoting a prediction time span of 1; 'indicators_num' is set to 4, signifying the four meteorological drought indicators utilised in this study; 'longitude' and 'latitude' represent the spatial dimensions of the study region, each dimension having a value of 256. Detailed dimensional transformations at each stage of the encoder–decoder process are illustrated in Fig. 2. The model was trained on an NVIDIA A100 GPU using the AdamW optimiser. The initial learning rate is set to 1×10^{-4}. However, the learning rate is not constant throughout training and is instead dynamically reduced according to the model's learning progress. In addition, common data augmentation techniques, including flip, rotation and Gaussian noise, are leveraged to further bolster the efficacy of model training.

3. Results

3.1 Overall prediction performance evaluation

The study period in Table 2 encompasses the entirety of the year 2020. We employ root mean square error (RMSE) and correlation coefficient (r) as performance evaluation metrics to gauge the forecasting accuracy. A well-performing model is indicated by an RMSE close to 0 and r close to 1. These statistical outcomes are juxtaposed with those computed from ERA5 data to exhibit the comprehensive performance of SPI30, SPI90, SPEI-1 and SPEI-3 across the entirety of East Asia.

Table 2 Comprehensive assessment of prediction accuracy

Parameter	SPI30	SPI90	SPEI-1	SPEI-3
RMSE	0.6011	0.5366	0.5343	0.5076
r	0.5672	0.6609	0.7947	0.7905

Table 2 indicates that the average RMSEs for all indices hover within the range of 0.5–0.6, with SPI30 recording the highest and SPEI-3 the lowest. This discrepancy can be attributed to meteorological drought being a complex, nonlinear phenomenon that transpires on disaster scales.

Employing shorter time windows captures abundant drought-related information, albeit at the cost of increasing prediction difficulty. Indices with extended time windows, such as SPEI-3, portray meteorological drought evolution on a seasonal scale by disregarding short-term anomalies, thereby resulting in a relatively stable overall trend and improved prediction accuracy.

Conversely, SPI is derived using a daily-progress methodology that ensures timely updates of prediction results but may compromise some degree of precision. Consequently, more reliable indices should be selected as the primary reference based on specific application requirements within the limits of acceptable accuracy. Other indices can function as subsidiary indicators to facilitate a comprehensive evaluation of meteorological drought.

The average *r* results generally echo the overall trend presented by the RMSE, with long-term predictions showing a higher correlation with the labels. Nonetheless, a notable difference lies in the fact that SPEI's average *r* typically exceeds that of SPI. This finding indirectly suggests that while the progressive-based daily scale can capture abundant information, it equally increases the complexity of prediction.

3.2 Spatial pattern

This study achieves spatiotemporal prediction of meteorological drought across multiple indices and time scales. A more nuanced analysis is warranted following an evaluation of the overall accuracy of these predictions. We begin by selecting prediction results from two distinct starting dates in winter and summer for a more visually engaging illustration.

Fig. 3 maps out spatial patterns for prediction results with starting dates on 21 February 2020 and 16 September 2020, respectively. Predictions for the four drought indicators, namely SPI30, SPI90, SPEI-1 and SPEI-3, align closely with the label results in terms of overall spatial patterns. Negative areas signify drought, and positive areas indicate wetness, considering the definition of drought in Table 1. The spatial maps abut drought–wetness areas offers a more precise delineation of regional drought intensity and extent.

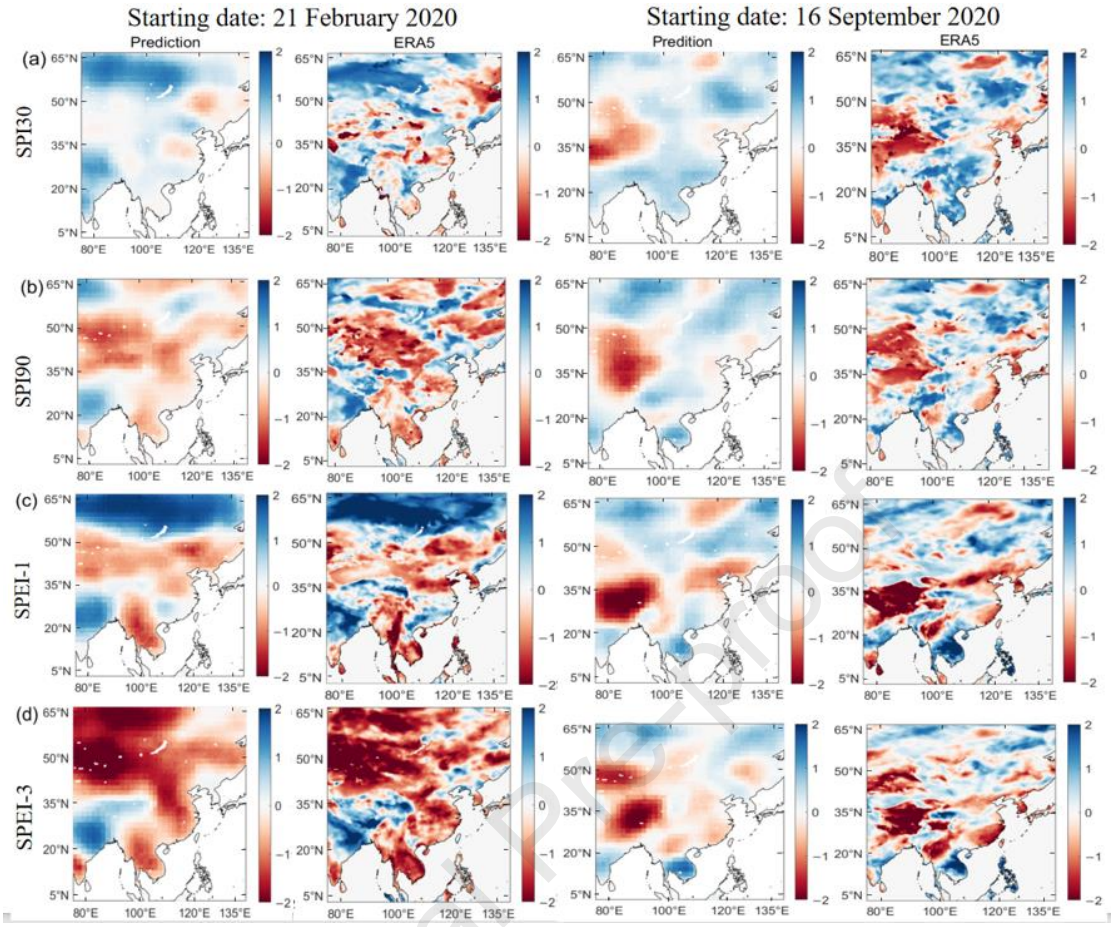

Fig. 3. Comparative spatial patterns of drought predictions with varied starting dates, (a) SPI30, (b) SPI90, (c) SPEI-1 and (d) SPEI-3.

For instance, predictions corresponding to the start date of 16 September 2020 accurately pinpoint a prominent drought event on the western side of the study area. Different from meteorological station-based observations, predictions with a spatial structure not only identify the occurrence of drought but also adequately capture its spatial coverage. This finding proves crucial for effective drought prevention measures and mitigation of related natural disasters.

Moreover, multiscale prediction results can effectively track the evolution of meteorological drought. For example, the shift in drought ranges within 30–90 d in the SPI30 and SPI90 predictions starting 21 February 2020, moving from a northeasterly to a westerly position, is clearly depicted. The progression of meteorological drought from short-term to long-term is revealed, owing to the inclusion of multiple time scales. This condition underlies the importance of accurate multiscale predictions in tracking drought evolution. Fig. 3 also shows the discrepancies in detailed coverage and intensity between SPI and SPEI results. Consequently, utilising multiple indicators can effectively generate more balanced and accurate drought predictions.

3.3 Temporal evolution

Upon spatial pattern analysis, we narrow our focus to two characteristic mountain ranges in East Asia, namely, the Kunlun and Himalayas Mountains. A comparative analysis is undertaken on drought conditions within these focal regions, taking into account temporal changes in drought (Fig. 4).

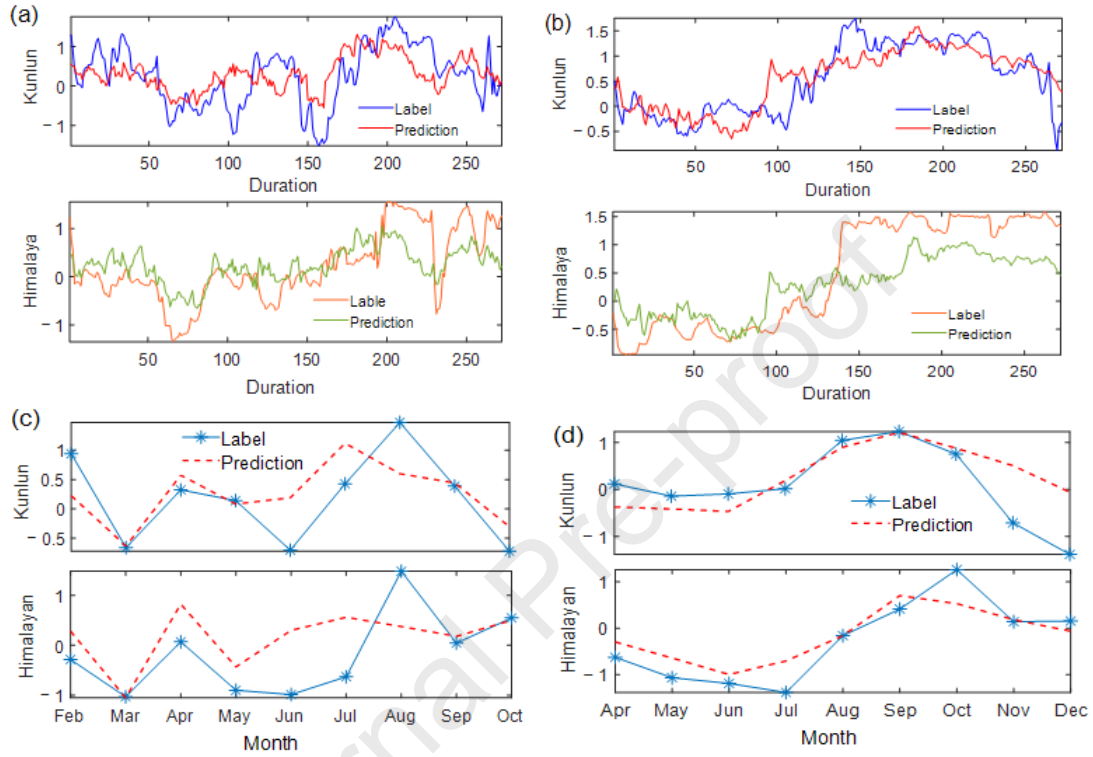

Fig. 4. Time series of prediction results of the Kunlun Mountains and the Himalayas Mountains, (a) SPI30, (b) SPI90, (c) SPEI-1 and (d) SPEI-3.

As depicted in Fig. 4, the SPI and SPEI predictions correspond with the labels regarding the overall trend. The finding suggests that the proposed multiscale framework yields superior predictive skill across the four timescales, capably tracking drought evolution over time. SPI30 and SPI90 predictions align closely with labelled values over certain periods. However, some intervals show less overlap. Despite this condition, the overall trend is generally consistent, particularly in the case of SPI90 predictions, attributable to longer windows smoothing short-term anomalous fluctuations.

Evident divergences are observed between prediction outcomes and label values on certain days, as illustrated in Fig. 4a and b. For instance, negative label values, which serve as an indication of drought, are observed around day 100 in the Kunlun region and day 125 in the Himalayan region. By contrast, predicted values fail to reflect this drought variation, occasionally even suggesting a different trend. Fig. 4b demonstrates that the model inadequately represents an wet phase starting around day 150 in the Himalayan Mountains. The SPEI predictions featured in Fig. 4c and d employ a monthly scale compared with SPI's daily time scale. This approach fails to capture rapid drought–wetness changes but is more effective in representing long-term and monthly scale trend variations.

3.4 Prediction skill in typical drought events

The primary objective of model prediction is to anticipate meteorological drought occurrences, thereby facilitating proactive steps to mitigate corresponding natural disasters, particularly in regions with a dearth of observational data. Our analysis leverages prediction results to scrutinise three distinct drought events that occurred or were triggered in 2020. This study aims to shed light on the practical implications of the proposed multiscale meteorological drought predictive model. Correspondingly, the results derived from ERA5 data are used for comparative validation. Fig. 5 showcases the outcomes of three handpicked characteristic drought events: flash drought, sustained drought and severe drought.

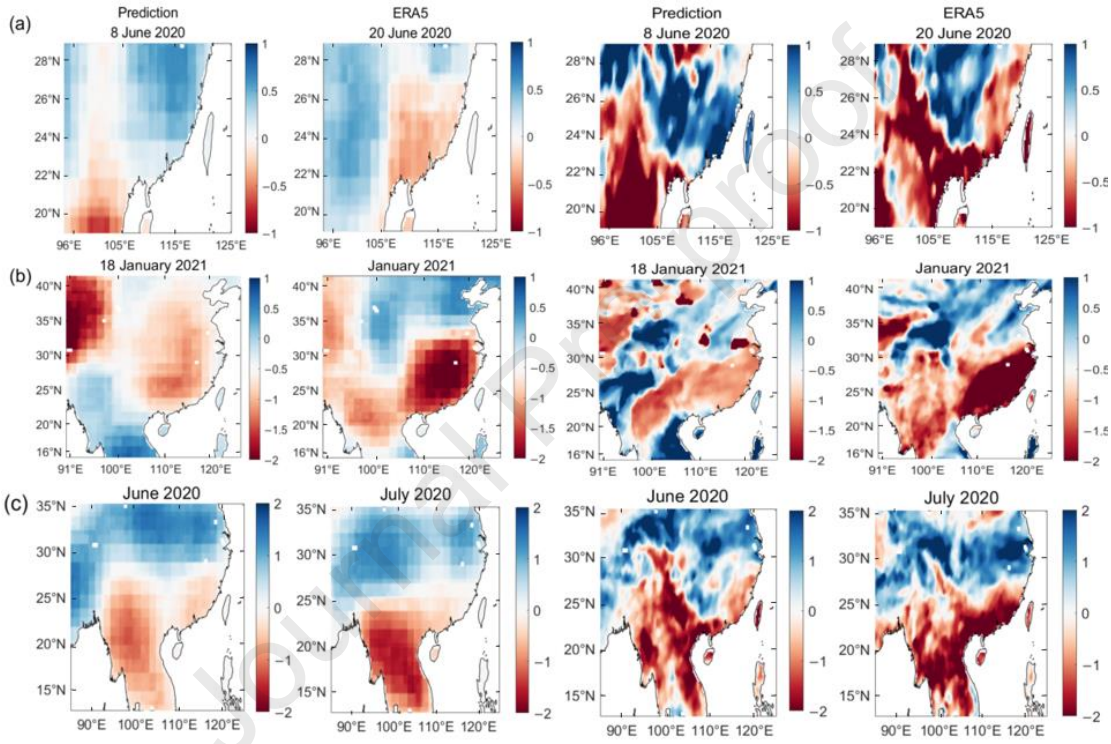

Fig. 5. Comparative results of three distinct drought events in 2020, (a) flash drought (indicated by SPI30 with a start date of 8 June and a peak date of 20 June, (b) sustained drought (indicated by SPI90 (first and three columns) and SPEI-3 (second and fourth columns) on January 2021), and (c) severe drought (indicated by SPEI-1 on June and July).

Flash drought, a rapidly occurring phenomenon, can seriously jeopardise ecosystems. However, long timescale indices often fall short in forecasting flash drought occurrences because of their sporadic nature (Dikshit et al., 2022). In this study, the multi-timescale prediction results, particularly the daily progression-based SPI30 predictions, not only pinpoint specific dates but also account for short-term anomalous variations overlooked by longer timescale predictions. Wang and Yuan (2022) detailed and analysed a flash drought event in southeastern China's coastal region, instigated by persistent high-pressure anomalies and dry land–air coupling. This flash drought event, spanning coordinates (20°–25°N, 111°–121°E)–(29°–24° N, 119°–109°E), ensued on 8 June 2020 and reached

its zenith on 20 June 2020. Fig. 5a illustrates that a large area centred around (23°N, 110°E) remained relatively humid initially. However, on 20 June, the SPI30 in this area had considerably declined into negative values, indicating a drought trend. The comparison between the model predictions and the ERA5 results evidently shows that the drought intensity predicted by the model is low. This finding indicates that the model may have limitations in accurately predicting short-term extreme changes. However, in general, the comparison in Fig. 5a confirms that short-term predictions can effectively designate the occurrence and coverage of flash droughts on specific days.

Fig. 5b depicts a sustained drought event in South China, commencing in winter 2020 and persisting until spring 2021 (Feng et al., 2022). We employ two long-time indicators, SPI90 and SPEI-3 for analysis, given the prolonged duration of sustained droughts. SPI90, calculated from precipitation accumulations over the past 90 d, can specify a particular date, whereas SPEI-3, obtained monthly, only indicates monthly forecast results. Fig. 5b clearly illustrates that long-timescale indicators predict the occurrence of this sustained drought event and relative coverage with reasonable accuracy, thereby corroborating the effectiveness and practicality of the model in indicating sustained drought events. Fig. 5b, also shows that the model predictions' intensity is lower than the label, and the drought intensity indicated by SPEI-3 is higher than SPI90. This discrepancy highlights the differences between indicators that consider temperature and precipitation variables (SPEI-3) versus indicators that solely rely on precipitation variables (SPI90). Therefore, using multiple indicators can mirror each other, ensuring objectivity in prediction results.

A severe drought in South China in June and July (Liu et al., 2022) is shown in Fig. 5c. We use SPEI-1 for analysis because the severe drought was caused by the Super East Asian monsoon, which occurred during the months of June–July and did not involve a specific start date. It can be seen in Fig. 5c, drought conditions are observed in southern China in June due to extreme precipitation anomalies over the East Asia–western Pacific, and the drought conditions in the region further intensified in July, which is consistent with the analysis described by Liu et al (2022).

4. Discussion

This study pioneers the introduction of the innovative concepts of multiple indices and multiple time scales in meteorological drought prediction. The deep learning-based intelligent prediction model satisfies the requirements for higher accuracy and spatiotemporal resolution in practical applications. This technique provides an effective data guarantee for meteorological drought-related research and disaster prevention in regions with scarce observational data, complex topography and diverse microclimate systems.

The overall prediction performance evaluation evidently shows that the errors and correlations between the predictions of the proposed model and the 'true' values derived by ERA5 data are

acceptable. The main advantages of using advanced deep learning architectures over traditional numerical simulation or statistical regression methods in solving hard-to-predict meteorological drought problems are as follows: multiple timescales and various meteorological drought indicators can be simultaneously considered; unknown and small-sample extreme events can be predicted without explicit intrinsic modelling laws; model architecture is flexible, and inference is efficient.

The results of spatial patten analysis demonstrate the differences between diverse predictors. These differences likely stem from the varying meteorological variables encompassing each indicator, coupled with diverse principles and mechanisms for drought's explanations, thereby yielding distinct results. SPI solely accounts for precipitation, precluding measurement of localised variations in evapotranspiration and soil moisture retention. It also lacks representations about the causes of drought and its evolutionary mechanisms, causing difficulty in achieving an adequate and objective evaluation of regions with complex climatic and geographic situations. By contrast, SPEI calculates potential evapotranspiration that incorporates air temperature, considering the evaporative process integral to drought onset. Therefore, when evaluating drought conditions within a region of concern, the ability to draw conclusions through integrations of contextual environmental attributes and multiple indicators exemplifies its superiority and practical worth. Moreover, comparative analyses of the two indices potentially elucidate drought drivers and mechanisms pertinent to areas under investigation.

Temporal evolution results showcase that short-term drought primarily stems from deficient precipitation, whereas long-term drought additionally correlates with diverse climatic and geographic influences beyond rainfall patterns. Within mountainous territories hosting microclimate systems and irregular topographies, obtaining observational data requires substantial expenditures of manpower and financial resources, limiting comprehensive representation across regions. Consequently, the dearth of flexible, effective and comprehensive coverage datasets holistically characterising meteorological drought poses a critical impediment to water resource administration and hazard mitigation efforts. While the experimental findings suggest that the proposed framework may not satisfactorily perform during some intervals, the results demonstrably discern the initiation and progression of drought states across mountainous locales from diverse temporal perspectives. These capabilities are exceptionally relevant to applications and investigations within this domain.

The analysis results of representative drought events illustrate the value of model predictions in practice. However, Fig. 5 shows only three typical drought events occurring in the study area, which cannot sufficiently verify the generalisability of most drought events. Given the limited number of documented typical drought events, the modelling region and study timeframe should be further expanded in the future to better validate the model predictions' universality.

Overall, the proposed model achieved excellent performance in capturing drought trend changes, impact coverages and evolution characteristics. However, several challenges remain to be addressed.

One challenge is the lag effect inherent in meteorological drought occurrences. As shown in Fig. 4c and d, predictions based on the monthly scale struggled with representing the latency effects of drought in a timely manner. Another challenge is the insufficiency in accurately capturing prediction intensity. Specifically, while the predictions anticipated future drought or humidity trends in target areas reasonably well, the exact severity levels are not precisely represented, especially during periods of large fluctuations, as illustrated in Fig. 3.

In addition, short-term anomalous variations posed difficulty for model predictions. Such discrepancies could arise from transient drought phenomena underrepresented in the training data because of their sporadic nature. Moreover, extreme precipitation events could induce sudden wetness anomalies within brief periods, severely limiting the model's ability to deliver accurate predictions when faced with abrupt changes triggered by such situations.

Despite certain challenges and limitations, the proposed multiscale drought model demonstrates promising capabilities for drought prediction in East Asia. It serves as a relatively effective supplementary method when observational data are insufficient. The use of gridded meteorological data products enables region-wide predictions without limitations posed by the location and distribution of meteorological observation stations. This study focuses on meteorological drought modelling within East Asia, the geographic characteristics and climate change of which are typical. Therefore, the results of the study can not only fully validate the performance of the model but also largely prove its universal application values. In addition, as the causes and changing mechanisms of meteorological drought are complex nonlinear processes, adopting multi-scale predictive model not only provides an effective means of obtaining data, but also lays the foundation for studying the temporal evolution processes and underlying mechanisms related to drought.

5. Conclusions

We developed a spatiotemporal deep learning model, leveraging ERA5, a well-recognised high-resolution gridded climatic product, to predict meteorological drought in East Asia. The proposed deep learning model employs a Swin transformer infrastructure to extract more effective semantic information and spatiotemporal properties through a window-based attention mechanism.This approach generates extensive and accurate spatiotemporal predictions.

The overall temporal and spatial accuracy results suggest that all index predictions are within an acceptable range. The daily-progress SPI30 results have the lowest accuracy, exhibiting an average RMSE and *r* value of 0.6011 and 0.5672, respectively. The highest overall accuracy is achieved by the monthly-progress, seasonal-scale SPEI-3, outperforming SPI30 by 15.6% in average RMSE and 18.2% in average *r*. Furthermore, specific dates in summer and winter are analysed, demonstrating the prediction's reasonable effectiveness at indicating the spatial region and extent of drought events. Our

spatial analysis identified two typical high mountain regions in East Asia for further precision analysis from a temporal perspective and revealed areas of insufficiency in prediction intensity and poor results in short-term abnormal changes. In addition, the analysis of three distinct drought events that occurred in 2020 revealed that multi-timescale predictions can be flexibly applied to scenarios with varying characteristics.

Declaration of competing interest

The authors declare no conflict of interest.

CRediT authorship statement contribution

Jia-Li Zhang: Conceptualisation, Methodology, Software, Formal analysis, Visualisation, Writing – original draft. Xiao-Meng Huang: Conceptualization, Supervision, Funding acquisition, Writing – review & editing. Yu-Ze Sun: Investigation, Data curation, Visualisation, Validation.

Acknowledgments

This work is supported by the National Key Research and Development Program of China (2022YFE0195900, 2021YFC3101600, 2020YFA0607900, and 2020YFA0608000) and the National Natural Science Foundation of China (42125503 and 42075137).

References:

Acharki, S., Singh, S.K., do Couto, E.V., et al., 2023. Spatio-temporal distribution and prediction of agricultural and meteorological drought in a Mediterranean coastal watershed via GIS and machine learning. Phys. Chem. Earth, Parts A/B/C 131, 103425. https://doi.org/https://doi.org/10.1016/j.pce.2023.103425.

Alsubih, M., Mallick, J., Talukdar, S., et al., 2021. An investigation of the short-term meteorological drought variability over Asir Region of Saudi Arabia. Theor. Appl. Climatol. 145, 597–617. https://doi.org/10.1007/s00704-021-03647-4.

Azimi, S.M.E., Sadatinejad, S.J., Malekian, A., et al., 2023. Application of artificial intelligence hybrid models for meteorological drought prediction. Nat. Hazards 116, 2565–2589. https://doi.org/10.1007/s11069-022-05779-w.

Danandeh Mehr, A., Rikhtehgar Ghiasi, A., Yaseen, Z.M., et al., 2023. A novel intelligent deep learning predictive model for meteorological drought forecasting. J. Ambient Intell. Humaniz. Comput. 14, 10441–10455. https://doi.org/10.1007/s12652-022-03701-7.

Dikshit, A., Pradhan, B., Huete, A., 2021. An improved SPEI drought forecasting approach using the long short-term memory neural network. J. Environ. Manage. 283, 111979.

https://doi.org/https://doi.org/10.1016/j.jenvman.2021.111979.

Dikshit, A., Pradhan, B., Santosh, M., 2022. Artificial neural networks in drought prediction in the 21st century: a scientometric analysis. Appl. Soft Comput. 114, 108080. https://doi.org/10.1016/j.asoc.2021.108080.

Duan, S., Zhang, X., 2022. AutoML-based drought forecast with meteorological variables 1–5.

Feng, W., Leung, M.Y.T., Wang, D., Zhou., et al, 2022. An extreme drought over South China in 2020/21 concurrent with an unprecedented warm Northwest Pacific and La Niña. Adv. Atmos. Sci. 39, 1637–1649. https://doi.org/10.1007/s00376-022-1456-0.

Hao, Z., Singh, V.P., Xia, Y., 2018. Seasonal drought prediction: advances, challenges, and future prospects. Rev. Geophys. 56, 108–141. https://doi.org/10.1002/2016RG000549.

Huang, L., Wang, S., Jiang, K., Huang, J., 2022. GMA: an improved framework of radar extrapolation based on spatiotemporal sequence neural network. Earth Sp. Sci. 9. https://doi.org/10.1029/2022EA002502.

Jamei, M., Ahmadianfar, I., Karbasi, M.,et al., 2023. Development of wavelet-based kalman online sequential extreme learning machine optimized with boruta-random forest for drought index forecasting. Eng. Appl. Artif. Intell. 117, 105545. https://doi.org/10.1016/j.engappai.2022.105545.

Kitoh, A., 2004. Effects of mountain uplift on East Asian summer climate investigated by a coupled atmosphere-ocean GCM. J. Clim. 17, 783–802. https://doi.org/10.1175/1520-0442(2004)017<0783:EOMUOE>2.0.CO;2.

Lavaysse, C., Vogt, J., Toreti, A., et al., Pappenberger, F., 2018. On the use of weather regimes to forecast meteorological drought over Europe. Nat. Hazards Earth Syst. Sci. 18, 3297–3309. https://doi.org/10.5194/nhess-18-3297-2018.

Liu, C., Hu, C., Yang, S., et al., 2022. Super East Asian monsoon Mei-yu in June and July 2020 tied to dissimilar-shifting upper-level westerlies. Atmos. Res. 274, 106213. https://doi.org/10.1016/j.atmosres.2022.106213

Li, J., Wang, Z., Wu, X., et al., 2021. Robust meteorological drought prediction using antecedent SST fluctuations and machine learning. Water Resour. Res. 57, 1–20. https://doi.org/10.1029/2020WR029413

Liu, Z., Lin, Y., Cao, Y., et al., 2021. Swin transformer: Hierarchical vision transformer using shifted windows. Proc. IEEE Int. Conf. Comput. Vis. 9992–10002. https://doi.org/10.1109/ICCV48922.2021.00986

Liu, Z., Ning, J., Cao, Y., et al., 2022. Video swin transformer. Proc. IEEE Comput. Soc. Conf. Comput. Vis. Pattern Recognit, pp. 3192–3201. https://doi.org/10.1109/CVPR52688.2022.00320.

Manzano, A., Clemente, M.A., Morata, A., et al., 2019. Analysis of the atmospheric circulation pattern

effects over SPEI drought index in Spain. Atmos. Res. 230, 104630. https://doi.org/https://doi.org/10.1016/j.atmosres.2019.104630.

Martens, B., Schumacher, D.L., Wouters, H., et al., 2020. Evaluating the land-surface energy partitioning in ERA5. Geosci. Model Dev. 13, 4159–4181. https://doi.org/10.5194/gmd-13-4159-2020.

Minixhofer, C., Andreadis, P., Swan, M., Mcmeekin, C., 2021. DroughtED: A dataset and methodology for drought forecasting spanning multiple climate zones SmartSociety-Hybrid and diversity-aware collective adaptive systems view project

Mishra, A.K., Singh, V.P., 2010. A review of drought concepts. J. Hydrol. 391, 202–216. https://doi.org/https://doi.org/10.1016/j.jhydrol.2010.07.012.

Mo, K.C., Lyon, B., 2015. Global meteorological drought prediction using the North American multi-model ensemble. J. Hydrometeorol. 16, 1409–1424. https://doi.org/10.1175/JHM-D-14-0192.1

Rashid, M.M., Sharma, A., Johnson, F., 2020. Multi-model drought predictions using temporally aggregated climate indicators. J. Hydrol. 581, 124419. https://doi.org/https://doi.org/10.1016/j.jhydrol.2019.124419.

Rhee, J., Im, J., 2017. Meteorological drought forecasting for ungauged areas based on machine learning: using long-range climate forecast and remote sensing data. Agric. For. Meteorol. 237–238, 105–122. https:// doi.org/10.1016/j.agrformet.2017.02.011.

Shen, R., Huang, A., Li, B., Guo, J., 2019. Construction of a drought monitoring model using deep learning based on multi-source remote sensing data. Int. J. Appl. Earth Obs. Geoinf. 79, 48–57. https://doi.org/https://doi.org/10.1016/j.jag.2019.03.006.

Torres-Vázquez, M.Á., Halifa-Marín, A., Montávez, J.P., et al., 2023. High resolution monitoring and probabilistic prediction of meteorological drought in a Mediterranean environment. Weather Clim. Extrem. 40, 0–9. https://doi.org/10.1016/j.wace.2023.100558.

Tyagi, S., Zhang, X., Saraswat, D., et al., 2022. Flash drought: Review of concept, prediction and the potential for machine learning, deep learning methods. Earth's Futur. 10, 1–19. https://doi.org/10.1029/2022EF002723.

Vaswani, A., Shazeer, N., Parmar, N.,et al., 2017. Attention is all you need. Advances in neural information processing systems, 30.

Vicente-Serrano, S.M., Beguería, S., López-Moreno, J.I., 2010. A multiscalar drought index sensitive to global warming: The standardized precipitation evapotranspiration index. J. Clim. 23, 1696–1718. https://doi.org/10.1175/2009JCLI2909.1.

Wang, Y., Yuan, X., 2022. The anthropogenic acceleration and intensification of flash drought over the southeastern coastal region of China will continue into the future. Atmos. Ocean. Sci. Lett. 15, 100262. https://doi.org/10.1016/j.aosl.2022.100262.

524 Wu, Z., Yin, H., He, H., et al., 2022. Dynamic-LSTM hybrid models to improve seasonal drought
525 predictions over China. J. Hydrol. 615, 128706. https://doi.org/10.1016/j.jhydrol.2022.128706
526 Xin, Y., Lu, N., Jiang, H., et al., 2021. Performance of ERA5 reanalysis precipitation products in the
527 Guangdong-Hong Kong-Macao greater Bay Area, China. J. Hydrol. 602, 126791.
528 https://doi.org/https://doi.org/10.1016/j.jhydrol.2021.126791.
529 Zhang, X., Duan, Y., Duan, J., et al., 2022. A daily drought index-based regional drought forecasting
530 using the Global Forecast System model outputs over China. Atmos. Res. 273, 106166.
531 https://doi.org/10.1016/j.atmosres.2022.106166.

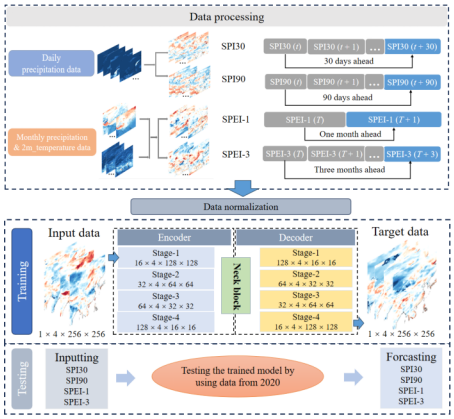

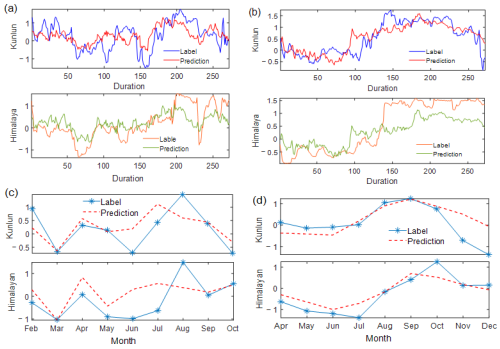

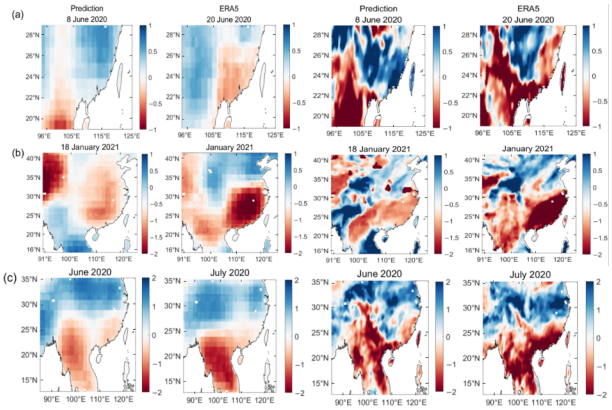

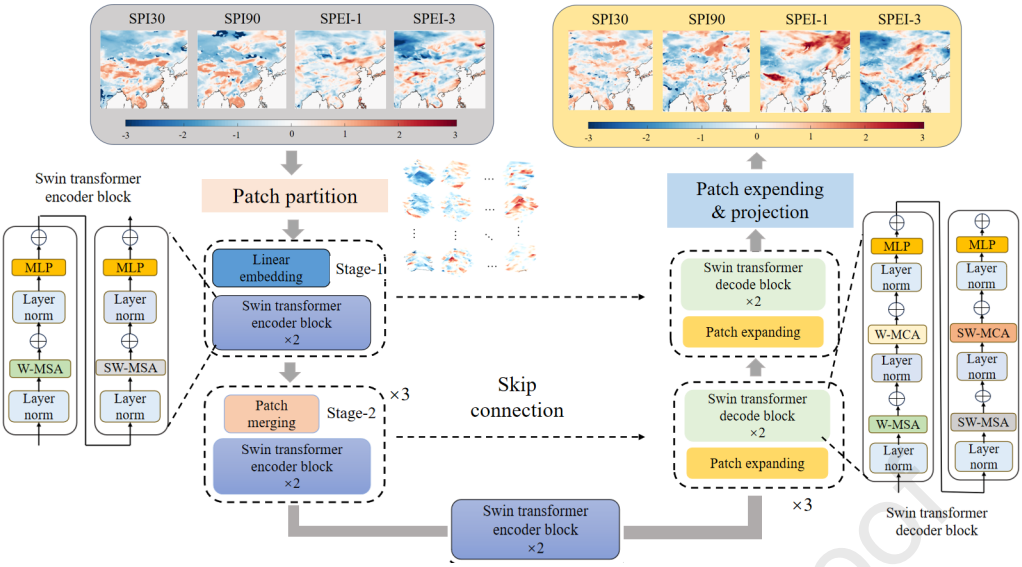

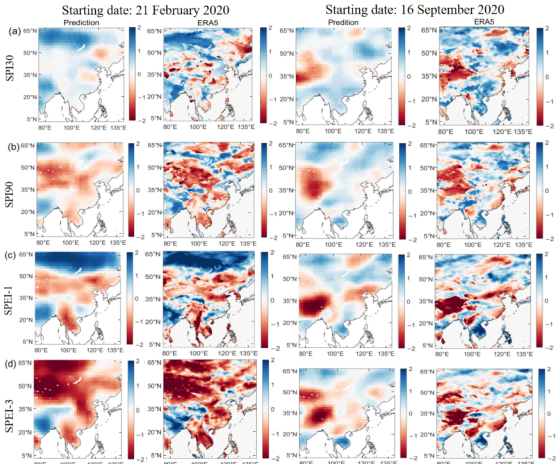

Declaration of competing interest

The authors declare no conflict of interest.